Available online at www.sciencedirect.com
SCIENCE DIRECT®
Thermochimica Acta 418 (2004) 3–9
thermochimica acta
www.elsevier.com/locate/tca

Characterisation of Lewis and Brønsted acidic sites in H-MFI and H-BEA zeolites: a thermodynamic and ab initio study

C. Busco [a,*], A. Barbaglia [b], M. Broyer [b], V. Bolis [c], G.M. Foddanu [d], P. Ugliengo [a]

[a] *Dipartimento di Chimica IFM Università di Torino and INSTM (Consorzio Interuniversitario Nazionale per la Scienza e Tecnologia dei Materiali) Unità di Torino, Via P. Giuria 7, 10125 Turin, Italy*
[b] *DiSCAFF Università del Piemonte Orientale "A. Avogadro", Via Bovio 6, 28100 Novara, Italy*
[c] *DiSCAFF Università del Piemonte Orientale "A. Avogadro" and INSTM (Consorzio Interuniversitario Nazionale per la Scienza e Tecnologia dei Materiali) Unità del Piemonte Orientale, Via Bovio 6, 28100 Novara, Italy*
[d] *Dipartimento di Chimica IFM Università di Torino, Via P. Giuria 7, 10125 Turin, Italy*

Received 10 February 2003; received in revised form 10 October 2003; accepted 25 November 2003

Available online 19 March 2004

Abstract

Adsorption enthalpies of N_2, CO, CH_3CN and NH_3 on H-BEA and H-MFI zeolites have been measured calorimetrically at 303K in order to assess the energetic features of the various interactions occurring within the zeolite nanocavities, namely: (i) specific adsorption on Lewis and Brønsted acidic sites; (ii) H-bonding interactions with hydroxyl nests; (iii) dispersive forces interactions with the walls of the cavities (*confinement effects*). Confinement effects have been investigated on an all-silica MFI zeolite (silicalite). The interaction of the molecular probes with model clusters mimicking Lewis and Brønsted sites has been simulated at ab initio level. The combined use of the two different approaches allowed to discriminate among the different interactions contributing to the measured heat of adsorption ($-\Delta_{ads}H$). Whereas CO and N_2 single out contributions from Lewis and Brønsted acidic sites, CH_3CN and NH_3 are not preferentially adsorbed on Lewis sites, suggesting that the adsorption on Brønsted sites is competitive with Lewis sites. The zero-coverage heats of adsorption for the different probes on the various systems correlate well with the proton affinity (PA) of the molecular probes.

Keywords: Adsorption; Zeolites; Microcalorimetry; Ab initio calculations; Lewis acidity

1. Introduction

Proton-exchanged zeolites are widely used as heterogeneous solid catalysts for acid-catalysed reactions requiring (high) Brønsted acidity [1–4]. The acidic features of zeolites are indeed dominated by the presence of proton acidic $\equiv Si(OH)^+Al^-\equiv$ species, which are originated by the isomorphous substitution of some Si atoms by Al in the silica framework. A great deal of work has been devoted in the past decades to the characterisation of $\equiv Si(OH)^+Al^-\equiv$ species, and much about their structure and properties is known [5–9]. Whereas the Brønsted acidic sites population depends upon the Si/Al ratio, their acidic strength seems to depend on the structure of the three-dimensional network and on the local atomic environment of the site [4]. Unfortunately the quantitative characterisation of the acidic properties of the $\equiv Si(OH)^+Al^-\equiv$ species is not yet routinely available [10] for a number of reasons, among which the simultaneous presence in zeolitic systems of other sites active towards the probe molecules routinely used. Indeed, a far less understood feature of some zeolites (β-zeolite is a well known case [11,12]) is their ability to show also Lewis acidic properties. At variance with the detailed knowledge of the Brønsted features described above, little is known about the Lewis sites nature and structure. Lewis acidic sites are relevant in many catalytic processes (i.e., Friedel–Crafts reactions), acting as electron acceptor centres giving rise to charge transfer processes. For this reason, some authors associate Lewis acidity in zeolites with framework trigonal Al atoms, originated by the former Brønsted sites as a result of thermal dehydroxylation [13]. Conversely, other research groups have hypothesised that Lewis sites are made up of ex-

* Corresponding author. Tel.: +39-011-670-7142; fax: +39-011-236-7140.
E-mail address: claudia.busco@unito.it (C. Busco).

0040-6031/$ – see front matter © 2003 Elsevier B.V. All rights reserved.
doi:10.1016/j.tca.2003.11.050

traframework Al^{III} species, leached from the zeolites framework during severe chemical or thermal treatments which induce the well known dealumination processes [14–16]. The actual nature of the Lewis centres in zeolites is then still doubtful and one of the aims of the present work is to provide new insight in their structural and energetic features.

In order to characterise the acidic sites in the zeolites nanocavities, the interaction of four probe molecules of increasing basic strength (N_2, CO, CH_3CN and NH_3) with zeolites of different structure and Si/Al ratio has been studied by adsorption microcalorimetry at 303 K. The basic strength of the probes has been quantified on the basis of their proton affinity (PA) [17].

H-β zeolite (BEA structure [18,19]) has been investigated because it is particularly rich in Lewis centres, which are known to be mainly localised at the stacking faults between the two equally stable crystalline phases. An H-β zeolite is thus a prototype for Lewis-rich zeolites. Conversely, H-ZSM-5 zeolite (MFI structure [20]) has been chosen because it sports mainly Brønsted acidic sites [21], even though some fraction of defective Al species exhibiting Lewis acidity is present in the structure [22]. In addition to the specific interaction with the acidic centres each probe molecule is expected to interact through dispersive forces with the walls of the pores giving rise to the well known *confinement effect* [23,24]. H-ZSM-5, in virtue of its smaller pore size (≈5.6 Å) is expected to manifest a larger *confinement effect* than H-β (≈6.7 Å [23–25]). Such an effect has been quantitatively investigated in the present work by adsorbing the probes on an Al-free defective MFI zeolite (silicalite [26]), which contains abundant "hydroxyl nests" (framework defects due to Si atoms vacancies [27]) and external isolated silanols (SiOH groups terminating the crystals [28]), both characterised by mild Brønsted acidic properties.

For all considered probes the enthalpies of adsorption ($q = -\Delta_{ads}H$) have been measured for the three different zeolites as a function of increasing coverage. The reported heat values have, however, an intrinsic average meaning, in that they result from both the specific interaction with Lewis and Brønsted centres, and the non-specific dispersive interactions with the zeolite walls. In order to gauge the various contributions to the measured heats of adsorption, ab initio calculations of the binding energies (BE) of the probes with model clusters representative of both Lewis and Brønsted sites have also been performed.

2. Experimental

2.1. Materials

H-β zeolite (BEA, Si/Al = 9.8, Al/uc = 5.9), H-ZSM-5 (MFI, Si/Al = 15, Al/uc = 6.0), Na- and Al-free defective silicalite (MFI, Si/Al → ∞), kindly supplied by *Polimeri Europa*, *Novara*, *Italy*. All samples have been vacuum activated ($p \leq 10^{-5}$ Torr, 14 h) at $T = 673$ K (H-ZSM-5 and silicalite) or $T = 873$ K (H-β), in order to achieve the maximum dehydration of the surface compatible with the stability of the structure.

2.2. Methods

2.2.1. Adsorption microcalorimetry

The heats of adsorption have been measured at 303 K by a heat-flow microcalorimeter (Calvet C80, Setaram) in order to evaluate the enthalpy changes related to the adsorption as a function of increasing coverage. A well-established stepwise procedure was followed [25,27,29,30]. The calorimeter was connected to a high vacuum ($p \leq 10^{-5}$ Torr) gas-volumetric glass apparatus, which enables to determine simultaneously the adsorbed amounts (n_{ads}) and the integral heats (Q^{int}) evolved for small increments of the adsorptive. The calorimetric data are reported in the present paper as *differential heats* ($q^{diff} = \delta Q^{int}/\delta n_{ads} = -\Delta_{ads}H$). The q^{diff} curves reported in the plots are the derivatives of the Q^{int} versus n_{ads} polynomial functions (not reported for the sake of brevity) which best fit the equilibrium data obtained, whereas the experimental points are the partial molar heats of adsorption defined as ($\Delta Q^{int}/\Delta n_{ads}$). These latter quantities are obtained by the experimental $\Delta Q^{int}/\Delta n_{ads}$ versus n_{ads} histogram [31]. The differential heat extrapolated to vanishing coverage ($q_0 = (-\Delta_{ads}H)_0$) represents the enthalpy change for the adsorption on the most energetic sites active in the early stage of the process. The pressure was monitored by a transducer gauge (Ceramicell 0–100 Torr, Varian).

2.2.2. Molecular modelling

All calculations have been run at ab initio level using the B3-LYP functional on selected molecular clusters modelling the different sites. For Lewis sites, in order to mimic the different geometrical strains around the *cus* Al^{III} likely present in the real material, two different clusters (LSC and LLC, Fig. 1) have been adopted; for the Brønsted site (BRO cluster, Fig. 1) one Si atom has been replaced by Al in a cluster cut out from the faujasite unit cell (adopted because of its geometrical rigidity). For calculations involving the LSC cluster, full B3-LYP/6-31 + G(d,p) geometry optimisation has been carried out, whereas for the LLC cluster, the ONIOM[B3-LYP/6-31 + G(d,p):MNDO] method [32] has been adopted to save computer resources. For the Brønsted site, either free or in interaction, full geometry optimisation with the ONIOM[B3-LYP/SVP:AM1] method has been carried out. The model regions, for both Lewis and Brønsted sites, are shown as balls and sticks in Fig. 1. For the ONIOM optimised structures, single point B3-LYP/6-31 + G(d,p) energy calculations have been carried out, from which binding energies, corrected for the basis set superposition error (BSSE), have been computed. N_2, CO (C-down) and CH_3CN (N-down) have been adsorbed on LSC, LLC and BRO model sites as "end-on" complexes, whereas NH_3 has been adsorbed on both model sites throughout the N atom. These arrangements are the most stable ones because they

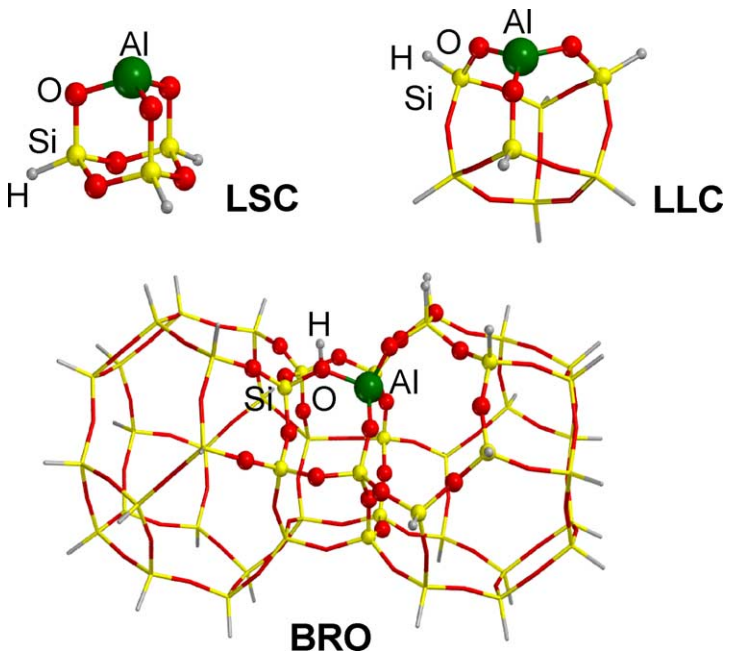

Fig. 1. Cluster models treated ab initio (LSC and LLC model: the Lewis site; BRO: the Brønsted site). Atoms shown as balls belong to the model region in the ONIOM calculation.

allow the most favourable charge-transfer process at Lewis sites and the linear geometry of the H-bonded complexes.

3. Results and discussion

3.1. Adsorption microcalorimetry

In Fig. 2 the differential heats of adsorption of N_2 (section a) and CO (section b) on H-β and H-ZSM-5 zeolites are reported as a function of the adsorbed amounts, in comparison with silicalite. The interaction of both probes with the nominally non acidic silicalite is very scarce, as witnessed by the low heat of adsorption ($q_{ads} \approx 14$ and 18 kJ/mol for N_2 and CO respectively) which is almost constant with coverage and can be taken as a measure of the *confinement effects* due to the dispersion forces in the zeolite cavities [25], vide infra. By contrast the interaction of the two probes with the acidic H-β and H-ZSM-5 zeolites is clearly stronger than with silicalite. The heats of adsorption decrease upon increasing coverage, as usual for heterogeneous surfaces. In the present case, the heterogeneity is due to the presence of, at least, two different families of sites, i.e., Brønsted and Lewis acidic sites of different strength. In the N_2 case, the low coverage enthalpy values show that on H-β a family of acidic sites slightly stronger than the H-ZSM-5 ones is present (approaching $q_0 \approx 45$ kJ/mol at vanishing coverage, see Fig. 2a). The differences in the energetic of the interaction between H-β and H-ZSM-5 are not relevant (the zero-coverage heat for this latter is ≈40 kJ/mol and the overall adsorption features for the two zeolites are quite similar), even though the population of Lewis acidic sites is more

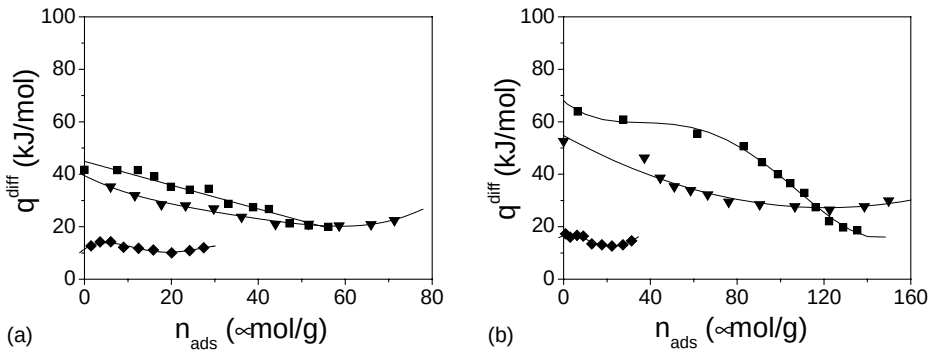

Fig. 2. Section (a): differential heats of adsorption (303 K) of N_2 on H-β (■), H-ZSM-5 (▼) and on defective silicalite (◆) reported as a function of the adsorbed amounts. Section (b): differential heats of adsorption (303 K) of CO on H-β (■), H-ZSM-5 (▼) and on defective silicalite (◆) reported as a function of the adsorbed amounts.

abundant on H-β than on H-ZSM-5 [25]. From computational data (vide infra), it turns out that the interaction energy of N_2 with the Brønsted site is negligible on an absolute scale. This means that, basically, only the contribution from the Lewis sites does affect the measured heat, particularly at vanishing coverage.

In the case of CO adsorption the heat versus coverage plots (see Fig. 2b) show remarkable differences between the two investigated acidic systems. In particular, even though the zero-coverage heat values are very close as for the N_2 adsorption ($q_0 \approx 60$ and 70 kJ/mol for H-ZSM-5 and H-β, respectively), the H-β values remain almost constant at $q \approx 60$ kJ/mol along a wide coverage interval, indicating the presence of relatively large amounts of defective Al^{III} species, available for σ-coordinating CO. This is confirmed by the enthalpy values (both zero- and low-coverage) which are compatible with the formation of $Al^{III} \leftarrow CO$ complexes on strong acidic sites [29].

By contrast, in the H-ZSM-5 case the q^{diff} versus n_{ads} curve rapidly decreases at increasing coverage and approaches a plateau at ≈30 kJ/mol. This latter value is typical of the formation of OC–H-bonded adducts on Brønsted $\equiv Si(OH)^+Al^-\equiv$ sites [33]. The fact that in the early stage of the adsorption the enthalpy values are larger than 30 kJ/mol confirms that in H-ZSM-5 a fraction of Lewis acidic sites is present, in agreement with what generally accepted for ZSM-5 materials [22] and with our IR-spectroscopic evidence (data not reported for the sake of brevity). These sites are both less abundant and less energetic on H-ZSM-5 than on H-β, suggesting a different nature (e.g., non-framework/framework, different geometrical strain) of the Al species in the two systems. The enthalpies of adsorption of CO cover a wide range of values from the zero-down to the high-coverage values (q_0 ≈20 and ≈30 kJ/mol for H-β and H-ZSM-5, respectively). The formation of H-bonded adducts on Brønsted sites (which involves a much lower energy of interaction than the coordination on Lewis sites) is favoured at high p_{CO} and apparently occurs on sites much more heterogeneous on H-β than on H-ZSM-5, for which a nearly constant heat of adsorption has been measured at high coverage (Fig. 2b). The process becomes eventually less energetic on H-β than on H-ZSM-5, which is characterised by a microporous system of smaller cavities, confirming that the *confinement effect* due to the influence of the walls of the cavities is more pronounced for the 10-membered MFI than for the 12-membered BEA structure. This is also witnessed by Ar adsorption, which has been found to be very weak and non-specific (opposite to what reported in ref. [34] for different systems) but involving a heat of adsorption lower for H-β than for H-ZSM-5 (16–7 kJ/mol and 27–14 kJ/mol, respectively, [25]).

The effect due to the presence of the nanocavities is energetically quantified by the nearly constant heat of adsorption of CO and N_2 on silicalite, in agreement with Savitz et al. [35] for CO adsorption at 195 K. The Na- and Al-free *defective* silicalite studied in the present work is much more reactive than expected for a *perfect* silicalite exposing only virtually inert SiOSi bridges in that the former contains abundant hydroxylated species (*hydroxyl nests*), available for H-bonding interactions [26,27].

Table 1
Experimental zero-coverage enthalpy of adsorption ($q_0 = (-\Delta_{ads}H)_0$) on H-β zeolite in comparison with ab initio BSSE corrected binding energies values, computed for the LSC and LLC clusters (models of the Lewis site) and for BRO cluster (model of the Brønsted site)

Probes	PA	$(-\Delta_{ads}H)_0$	LSC	LLC	BRO
N_2	494	45	56	38	6
CO	594	70	84	64	10
CH_3CN	779	115	173	134	36
NH_3	854	140	212	175	62

Gas phase proton affinities PA of the probe molecules are reported. All data in kJ/mol.

By comparing the adsorption of N_2 (Fig. 2a) and of CO (Fig. 2b) it is clearly evident that both energy of interaction and uptake are much larger for the latter, in agreement with the larger gas-phase proton affinity of CO (see Table 1). In order to check the influence of increasing the basic strength of the probe on the adsorption features, the zeolites under study were put in contact with CH_3CN (PA = 779 kJ/mol) and NH_3 (PA = 854 kJ/mol).

In Fig. 3 the differential heats of adsorption of CH_3CN (section a) and NH_3 (section b) on H-β and H-ZSM-5 are reported as a function of the adsorbed amounts, in comparison with silicalite. The heat of adsorption are in all cases much larger than for N_2 and CO. The zero-coverage values ($q_0 \approx 120$ kJ/mol for CH_3CN and ≈130 kJ/mol for NH_3, virtually identical for the two strongly acidic zeolites) are consistent with the formation of either protonated or strongly H-bonded species. For the weakly acidic silicalite the q_0 value is ≈60 kJ/mol for CH_3CN and ≈90 kJ/mol for NH_3. These values are much lower than those measured for the strongly acidic zeolites but it is worth noticing that they are significantly larger than the latent heats of liquefaction of the probes (30 and 21 kJ/mol for CH_3CN and NH_3, respectively). This result strongly suggests that the hydroxylated species present within the *defective* silicalite nanocavities are able to form stable H-bonded adducts.

The presence of Al atoms in the zeolite framework, either as $\equiv Si(OH)^+Al^-\equiv$ or *cus* Al^{III} species, is readily revealed by CH_3CN and NH_3 adsorption in that the heat versus coverage curves of H-β and H-ZSM-5 lie much above than the curves of the Al-free silicalite system. For CH_3CN this is true mostly in the early stage of the process (Fig. 3a) whereas for NH_3 the acidic zeolites curves are clearly distinguishable from silicalite in the whole coverage interval examined (Fig. 3b). The presence in the two acidic zeolites of Al atoms as $\equiv Si(OH)^+Al^-\equiv$ bridges or *cus* Al^{III} species is, however, not discriminated by the adsorption of CH_3CN or NH_3. The heat versus coverage plots of H-β and H-ZSM-5 are indeed very similar (CH_3CN) or virtually

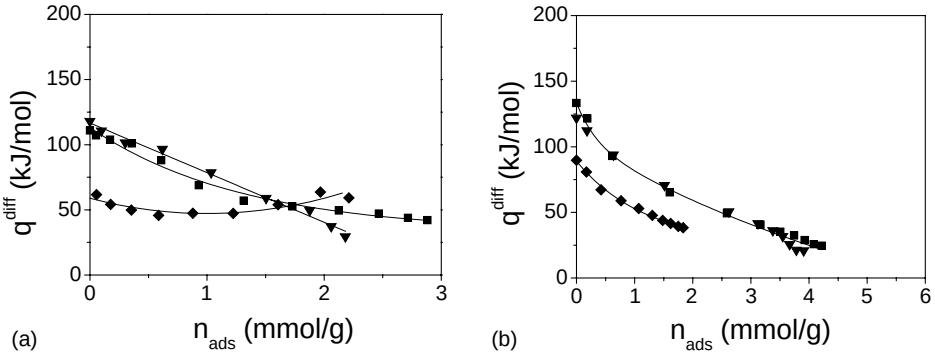

Fig. 3. Section (a): differential heats of adsorption (303 K) of CH_3CN on H-β (■), H-ZSM-5 (◆) and on defective silicalite (◆) reported as a function of the adsorbed amounts. Section (b): differential heats of adsorption (303 K) of NH_3 on H-β (■), H-ZSM-5 (▼) and on defective silicalite (◆) reported as a function of the adsorbed amounts.

coincident (NH_3), in spite of the different structure and distribution of Lewis and Brønsted sites in the two systems.

The reported results can be interpreted as follows: if the basic strength of the probe is low (as in the case of N_2 and CO) the interaction with the strongest sites (i.e., the Lewis ones) definitely prevails in the early stage of the adsorption process, and only at high coverage the interaction with Brønsted sites becomes competitive. If the basic strength of the probe is high enough to allow the formation of either protonated species, or strong H-bonded adducts (as in the case of both CH_3CN and NH_3, [12]) the interaction with Brønsted and Lewis sites is energetically competitive. This is particularly so, also in virtue of the larger proportion of Brønsted sites with respect to the Lewis ones.

In Fig. 4a the enthalpy of adsorption ($q_0 = (-\Delta_{ads}H)_0$) extrapolated at vanishing coverage has been contrasted with the gas-phase proton affinity of the probes adopted in the present work. The Ar adsorption datum, which has been discussed in ref. [25], has been added for comparison. A distinct behaviour is observed for the two strongly acidic zeolites with respect to the weakly acidic silicalite. In this latter case, indeed, for molecular probes with low PA (Ar, CO and N_2), the energy released is quite low (<25 kJ/mol) and very close to each other, because the interaction is dominated by dispersive forces, generated by the walls of the cavities. By contrast, for molecular probes of higher basic strength (CH_3CN and NH_3), the energy of interaction linearly increases with PA. For the acidic zeolites $(-\Delta_{ads}H)_0$ values increase linearly with PA for all molecular probes, according to the presence of specific Brønsted and Lewis acidic sites in the micropores.

3.2. Computational study

The contributions of Brønsted, Lewis, H-bonding and confinement effects to the measured $-\Delta_{ads}H$ are inextricably intermingled. In Fig. 4b an attempt has been made to single out the various component, by comparing the experimental differential heats of adsorption extrapolated to zero coverage ($q_0 = (-\Delta_{ads}H)_0$) measured for H-β zeolite with

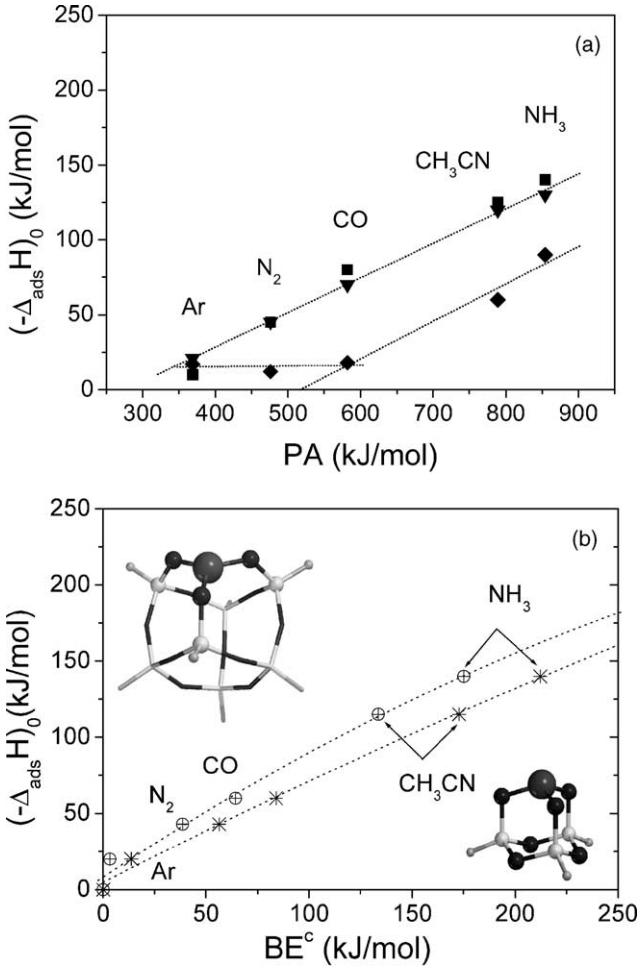

Fig. 4. Section (a): zero-coverage enthalpy of adsorption vs. proton affinity PA of the molecular probes for H-β (■), H-ZSM-5 (▼) and defective silicalite (◆). Section (b): zero-coverage enthalpy of adsorption on H-β zeolite vs. ab initio BSSE corrected binding energy, BE^C. Computed data for the LSC (⊛) and LLC (⊕) clusters, models of the Lewis site (as indicated in the figure).

the highest computed BE values, i.e., the ones for LSC and LLC Lewis models. Table 1 shows the PA values (gas phase proton affinities, kJ/mol) and the BSSE corrected binding energies (kJ/mol) for the complexes formed between the probe molecules and the Lewis and Brønsted models. In the same table the experimental $(-\Delta_{ads}H)_0$ for H-β zeolite are reported. As already anticipated, little is known about the structural and chemical nature of the Lewis sites in zeolites, so that two different models have been studied (LSC and LLC, Fig. 1) mimicking different geometrical constraints around the Al atom, apt to simulate different environment in the real material. The LSC cluster sports the highest sterical strain of the [AlO_3] moiety, the Si–O–Al angle being close to 110°. Because of that, the oxygen lone pairs can hardly be used to fill the Al unsatisfied valency, resulting in an enhanced Lewis acidic strength with respect to the LLC model, in which the Si–O–Al angle is around 145°. Indeed, the relevant binding energies are higher for the former than for the latter, according to the geometrical strain of the Al species. The BEs increase along the series N_2 < CO < CH_3CN < NH_3 for both models, in agreement with the PA values of the probes. The two sets of BE values for N_2 and CO on LSC and LLC models can be assumed as a possible energy range to which the experimental energetic data can be compared. For CO adsorbed on the Lewis-rich H-β zeolite, the $(-\Delta_{ads}H)_0$ value is ≈70 kJ/mol, which falls in between the two computed values (64 and 84 kJ/mol, for LLC and LSC, respectively). The same holds for N_2 adsorption, in that $(-\Delta_{ads}H)_0$ value is ≈45 kJ/mol, falling between LLC and LSC values (38 and 56 kJ/mol, respectively).

The energy of interaction of the probe molecules with the Brønsted site follows the same trend already found for the adsorption on the Lewis site, i.e., N_2 < CO < CH_3CN < NH_3. However, the BEs are by far much lower than those computed for the Lewis site. BE values for CO and N_2 resulted in 10 and 6 kJ/mol, respectively. These data strongly support the energy partition already proposed for the experimental values of the heats of adsorption. Indeed, for CO the difference in BE between the Lewis-LLC and the Brønsted site interaction ($\Delta(BE) = 54$ kJ/mol) is maximum, in agreement with what indicated by the H-β and H-ZSM-5 q^{diff} versus n_{ads} curves (see Fig. 2b). For N_2, the difference between the two sites is less pronounced ($\Delta(BE) = 32$ kJ/mol), in agreement with the similarity of the two experimental curves (see Fig. 2a). At this point we can stress that experimental and calculated data for N_2 and CO correlate well, showing that the largest contribution to the experimental $(-\Delta_{ads}H)_0$ is due to the Lewis interaction, as clearly indicated by the large gap between the ab initio BEs for LLC and BRO models. By contrast, the experimental values for the two polar probes (CH_3CN and NH_3) are lower than those computed for the Lewis sites showing that a sizable fraction of the energy is due to the interaction with Brønsted sites, which are in general weaker than the Lewis ones. This result is confirmed by the ab initio BEs on BRO sites the values of which are closer to the BEs for LLC site when compared to the cases of N_2 and CO, for which the Brønsted interaction contribution is negligible. Thus, in the real systems the energy of interaction of probes of high proton affinity such as CH_3CN and NH_3 does involve a significant contribution from the Brønsted sites.

4. Conclusions

The energetic features of the interaction of molecules with Brønsted and Lewis acidic sites, hydroxyl nests and with the cavity walls of microporous materials have been characterised by adsorption microcalorimetry and by ab initio cluster calculations simulating the interaction with the acidic sites. Namely, N_2 and CO single out mainly Lewis sites and are also sensitive to *confinement effects* due to dispersive forces which are governed by the micropores size. Polar molecules such as CH_3CN and NH_3 are not preferentially adsorbed on Lewis sites with respect to the Brønsted ones, in virtue of their ability to generate either protonated species or strong H-bonded adducts.

The experimental zero-coverage enthalpies correlate well with the proton affinities of the molecular probes, as well as with the binding energies calculated at ab initio level with model clusters mimicking Lewis *cus* Al^{III} acidic centres and Brønsted ≡$Si(OH)^+Al^-$≡ sites. Dispersive forces responsible for *confinement effects* in zeolite nanocavities were found to play a major role in stabilising the van der Waals adducts formed at the Lewis or Brønsted acidic sites as well as on hydroxylated species on defective silicalite.

Acknowledgements

This work was financially supported by the Italian MIUR (cofin 2000, coordinated by Professor A. Zecchina, Area 03: “Structure and reactivity of catalytic centers in zeolitic materials”) and by INSTM (progetto PRISMA 2002, coordinated by Professor C. Morterra: “Nanostructured oxidic materials for the adsorption and the catalysis”). Dr. G. Spanò and F. Rivetti (Polimeri Europa s.r.l. Centro Ricerche Novara Istituto G. Donegani Novara, Italy) are greatly acknowledged for kindly supplying the microporous samples studied in the present work, and Professors A. Zecchina and S. Bordiga (University of Turin, Italy) for fruitful discussions.

References

[1] A. Corma, Chem. Rev. 95 (1995) 559.
[2] A. Corma, A. Martinez, Adv. Mater. 7 (1995) 137.
[3] S.M. Csicsery, Pure Appl. Chem. 58 (1986) 841.
[4] W. Hölderlich, M. Hesse, F. Näumann, Angew. Chem. Int. Ed. Engl. 27 (1988) 226.
[5] A. Zecchina, C. Otero Arean, Chem. Soc. Rev. 187 (1997).
[6] E. Brunner, Catal. Today 38 (1997) 361.

[7] S. Coluccia, L. Marchese, G. Martra, Microporous Mesoporous Mater. 30 (1999) 43.
[8] A. Zecchina, C. Lamberti, S. Bordiga, Catal. Today 41 (1998) 169.
[9] R.J. Gorte, Catal. Lett. 62 (1999) 1.
[10] W.E. Farneth, R.J. Gorte, Chem. Rev. 95 (1995) 615.
[11] P.J. Kunkeler, B.J. Zuurdeeg, J.C. van der Waal, J.A. van Bokhoven, D.C. Koningsberger, H. van Bekkum, J. Catal. 180 (1998) 234.
[12] C. Pazè, S. Bordiga, C. Lamberti, M. Salvataggio, A. Zecchina, G. Bellussi, J. Phys. Chem. B 101 (1997) 4740.
[13] P.A. Jacobs, H.K. Beyer, J. Phys. Chem. 83 (1979) 1174.
[14] A. Pöppl, T. Rudolf, D. Michel, J. Am. Chem. Soc. 120 (1998) 4879.
[15] M.J. Remy, D. Stanica, G. Poncelet, E.J.P. Feijen, P.J. Grobet, J.A. Martens, P.A. Jacobs, J. Phys. Chem. 100 (1996) 12440.
[16] R.D. Shannon, K.H. Gardner, R.H. Staley, G. Bergeret, P. Gallezot, A. Auroux, J. Phys. Chem. 89 (1985) 4778.
[17] NIST Chemistry WebBook, Standard Reference Database Number, 69 July 2001, http://www.webbook.nist.gov/.
[18] J.B. Higgins, R.B. LaPierre, J.L. Schlenker, A.C. Rohrman, J.D. Wood, G.T. Kerr, W.J. Rohrbaugh, Zeolites 8 (1988) 446.
[19] G.H. Kuehl, H.K.C. Timken, Microporous Mesoporous Mater. 35–36 (2000) 521.
[20] G.T. Kokotailo, S.L. Lawton, D.H. Olson, W.M. Meier, Nature (Lond.) 272 (1978) 437.
[21] J.A. Dunne, M. Rao, S. Sircar, R.J. Gorte, A.L. Myers, Langmuir 12 (1996) 5896.
[22] M. Trombetta, G. Busca, S. Rossini, V. Piccoli, U. Cornaro, A. Guercio, R. Catani, R.J. Willey, J. Catal. 179 (1998) 581.
[23] R.J. Gorte, D. White, Microporous Mesoporous Mater. 35–36 (2000) 447.
[24] L. Yang, K. Trafford, O. Kresnawahjuesa, J. Sepa, R.J. Gorte, D. White, J. Phys. Chem. B 105 (2001) 1935.
[25] V. Bolis, M. Broyer, A. Barbaglia, C. Busco, G.M. Foddanu, P. Ugliengo, J. Mol. Catal. A, in press.
[26] S. Bordiga, I. Roggero, P. Ugliengo, A. Zecchina, V. Bolis, G. Artioli, C. Lamberti, J. Chem. Soc., Dalton Trans. (2000) 3921.
[27] V. Bolis, C. Busco, S. Bordiga, P. Ugliengo, C. Lamberti, A. Zecchina, Appl. Surf. Sci. 196 (2002) 56.
[28] J. Sauer, P. Ugliengo, E. Garrone, V.R. Saunders, Chem. Rev. 94 (1994) 2095.
[29] V. Bolis, G. Cerrato, G. Magnacca, C. Morterra, Thermochim. Acta 312 (1998) 63.
[30] V. Bolis, S. Bordiga, G. Turnes Palomino, A. Zecchina, C. Lamberti, Thermochim. Acta 379 (2001) 131.
[31] V. Bolis, S. Maggiorini, L. Meda, F. D'Acapito, G. Turnes Palomino, S. Bordiga, C. Lamberti, J. Chem. Phys. 113 (2000) 9248.
[32] S. Dapprich, I. Komaromi, K.S. Byun, K. Morokuma, M.J. Frisch, J. Mol. Struct. (Theochem.) 461–462 (1999) 1.
[33] S. Savitz, A.L. Myers, R.J. Gorte, J. Phys. Chem. B 103 (1999) 3687.
[34] H. Matsubashi, T. Tanaka, K. Arata, J. Phys. Chem. B 105 (2001) 9669.
[35] S. Savitz, A.L. Myers, R.J. Gorte, Microporous Mesoporous Mater. 37 (2000) 33.